



HAL
open science

Origin of Stereoselectivity in a Mechanochemical Reaction of Diphenylfulvene and Maleimide

Wakana Sakai, Lori Gonnet, Naoki Haruta, Tohru Sato, Michel Baron

► **To cite this version:**

Wakana Sakai, Lori Gonnet, Naoki Haruta, Tohru Sato, Michel Baron. Origin of Stereoselectivity in a Mechanochemical Reaction of Diphenylfulvene and Maleimide. *Journal of Physical Chemistry A*, 2023, 127 (28), pp.5790-5794. 10.1021/acs.jpca.3c01332 . hal-04163375

HAL Id: hal-04163375

<https://imt-mines-albi.hal.science/hal-04163375v1>

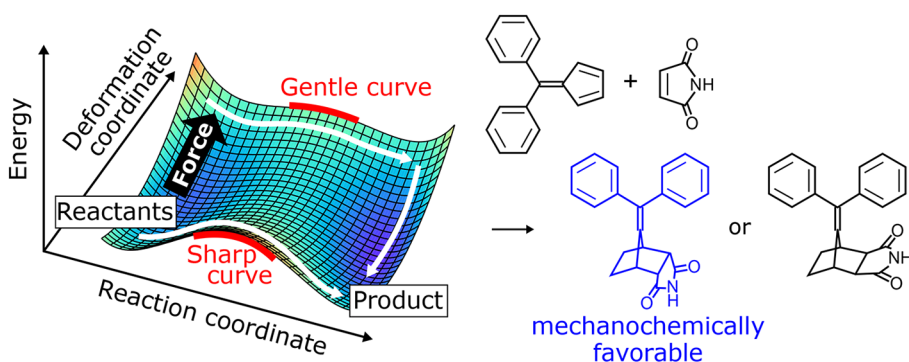
Submitted on 17 Jul 2023

HAL is a multi-disciplinary open access archive for the deposit and dissemination of scientific research documents, whether they are published or not. The documents may come from teaching and research institutions in France or abroad, or from public or private research centers.

L'archive ouverte pluridisciplinaire **HAL**, est destinée au dépôt et à la diffusion de documents scientifiques de niveau recherche, publiés ou non, émanant des établissements d'enseignement et de recherche français ou étrangers, des laboratoires publics ou privés.

Origin of Stereoselectivity in a Mechanochemical Reaction of Diphenylfulvene and Maleimide

Wakana Sakai, Lori Gonnet, Naoki Haruta, Tohru Sato,* and Michel Baron



ABSTRACT: Mechanochemical reactions sometimes yield unexpected products or product ratios in comparison to conventional reaction conditions. In the present study, we theoretically reveal the origin of the mechanochemical selectivity by considering the Diels–Alder reaction of diphenylfulvene and maleimide as an example. The application of an external force is equivalent to the production of a structural deformation. Here, we show that a mechanical force applied in a direction orthogonal to the reaction mode can lower the activation barrier by varying the potential energy curvature in the transition state. In the case of the Diels–Alder reaction, the *endo*-type pathway was found to be more mechanochemically favorable than the *exo*-type pathway, which is consistent with the experimental observations.

INTRODUCTION

Mechanochemical reactions are chemical reactions facilitated by mechanical actions such as ball milling,¹ mechanical pressure,² and ultrasound-induced polymer stress.³ Recently, these reactions have received considerable attention as novel synthetic methods because they do not require solvents or catalysts.⁴ In addition to the advantage of ecofriendliness, mechanochemical reactions also yield unexpected products and have selectivities, which are sometimes different from those under conventional solvent conditions. For example, Wang et al. reported that a high-speed vibration milling technique bridges buckminsterfullerenes, yielding a dumbbell-shaped C₁₂₀.⁵ Hickenboth et al. reported that, upon being subjected to ultrasound, polymeric substituents generate mechanical stress in cyclic compounds, facilitating ring-opening reactions, and the selectivities in these reactions could not be explained by the conventional Woodward–Hoffmann rules.⁶

Recently, Gonnet et al. reported a novel mechanochemical stereoselectivity in the Diels–Alder reaction of diphenylfulvene and maleimide, which generally yields two types of stereoisomers: *endo* and *exo* (see Figure 1).⁷ Under conventional toluene conditions, the *endo*-product yield is eight times higher than the *exo*-product yield. In contrast, the ball-milling

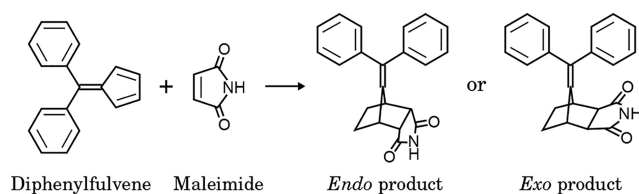


Figure 1. Diels–Alder reaction of diphenylfulvene and maleimide.

significantly increased the stereoselectivity: the *endo*-product yield was 46 times higher than the *exo*-product yield. The total yields also increased from 90% to 94%. The origin of these mechanochemical effects is still not well explained.

Theoretical approaches to mechanochemistry are now emerging.⁸ Most mechanochemical reactions are solid-state reactions. In ball milling, microcrystalline grains of reactants

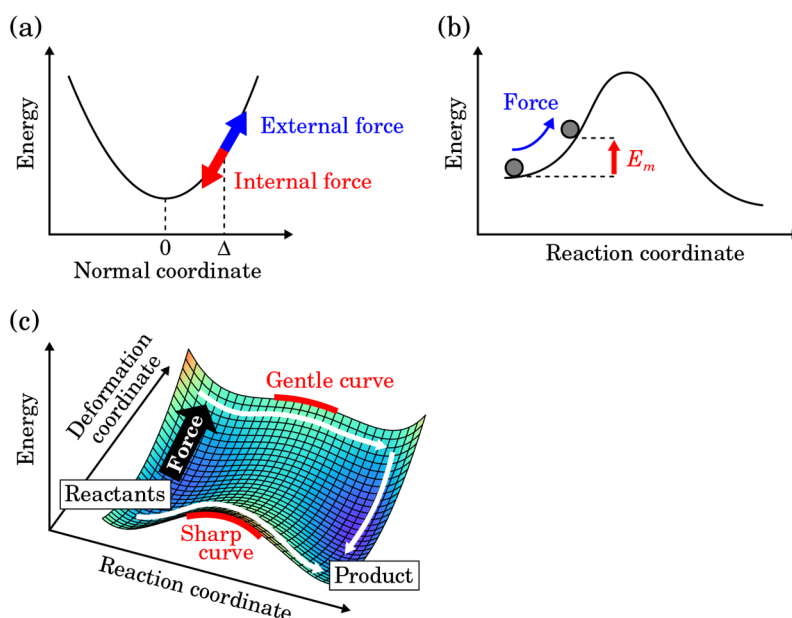


Figure 2. (a) Relation between a force and deformation in a potential energy curve. (b) Role of the force along the reaction mode. The external force provides a mechanical energy E_m that causes the reaction to progress. (c) Role of the force in a direction orthogonal to the reaction mode. The activation energy is lowered when the force changes the curvature at the TS.

are ground by hard balls in a reactor. The random impact of balls is transmitted to molecules at the interface of the grains via inter- and intramolecular deformations in the grains. Luty et al. discussed the impact of mechanical force on the electronic structure of reactant molecules via structural deformation, i.e., the inverse Jahn–Teller effect.⁹ Additionally, Ribas-Arino et al. proposed that a mechanical force can alter a reaction barrier by modifying the potential energy surface which can be regarded as a Legendre transformation from a point to a force.¹⁰ They explained the facilitation of the ring-opening reaction of *cis*-1,2-dimethylbenzocyclobutene under mechanochemical conditions. Furthermore, Haruta et al. found that a mechanical force can change a higher-order saddle point into a transition state (TS), thereby providing a new reaction path in the ball-milling process.¹¹ They reasonably explained the kinetics observed in the mechanochemical synthesis of dibenzophenazine. However, theoretical insights into the mechanochemical reactions are still limited. The origin of the mechanochemical selectivities typified by the Diels–Alder reaction of diphenylfulvene and maleimide has not yet been elucidated.

This study aims to clarify the influence of mechanical actions such as ball milling on selectivity from a quantum chemical viewpoint by considering the Diels–Alder reaction of diphenylfulvene and maleimide.

THEORY

During mechanical grinding, a random external force is applied to each reactant molecule because of the interfacial stacking of microcrystalline grains. Any external force acting on a molecule can be divided into its components along normal modes, similar to an internal force. Let us suppose that the applied force is mechanically balanced with the internal force,

$$F_\alpha + \left(\frac{\partial E}{\partial Q_\alpha} \right)_{Q_\alpha=\Delta} = 0 \quad (1)$$

where Q_α denotes a normal coordinate along mode α , and E represents the potential energy. As shown in Figure 2a, the application of force F_α for mode α is equivalent to performing a structural deformation of $Q_\alpha = \Delta$.

We briefly discuss the differences between mechanochemical and conventional conditions. Both conditions give rise to structural deformations (i.e., vibrational excitations), but these excited states are not the same. Under conventional conditions, all vibrational modes are excited according to the Boltzmann distribution. Thus, it is difficult for the thermal energy to realize a highly excited state. In contrast, under mechanochemical conditions, only specific modes are excited by a random force at a particular moment. The mechanical forces are momentarily comparable to the considerable thermal energy for these modes.

Herein, force directions are categorized into two types: the reaction mode and the other modes orthogonal to the reaction mode. First, we focus on the reaction mode. As shown in Figure 2b, an external force along the reaction mode facilitates the reaction progress. Hence, the thermal energy needed to overcome the reaction barrier is reduced by mechanical energy E_m . Thus, such a force could be one of the origins of an increase in yield under mechanochemical conditions. Furthermore, the Arrhenius equation is employed to determine the selectivity. The reaction rate constant k^P ($P = \text{endo}, \text{exo}$) is written as

$$k^P = A^P \exp\left(-\frac{E_a^P}{k_B T}\right) \quad (2)$$

where A^P is a frequency factor, E_a^P denotes the activation energy, k_B is the Boltzmann constant, and T is the temperature. When an external force along the reaction mode reduces the activation energy by E_m^P , the corresponding rate constant \tilde{k}^P is given by

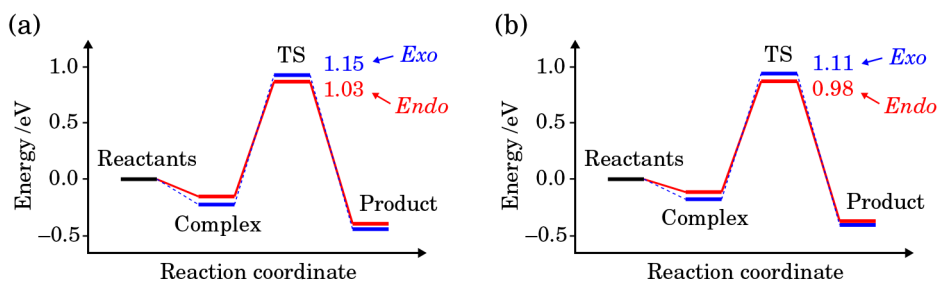


Figure 3. Energy diagrams of the Diels–Alder reaction of diphenylfulvene and maleimide (a) in a vacuum and (b) in toluene at the B3LYP/6-311G(d,p) level of theory. The solvent effect was incorporated by PCM. Values adjacent to the TSs indicate activation energies in eV.

$$\tilde{k}^P = A^P \exp\left(-\frac{E_a^P - E_m^P}{k_B T}\right) \quad (3)$$

Consequently, the ratio of the rate constants yielding *endo* and *exo* products is given by

$$\frac{\tilde{k}^{endo}}{\tilde{k}^{exo}} = \frac{k^{endo}}{k^{exo}} \exp\left(\frac{E_m^{endo} - E_m^{exo}}{k_B T}\right) \quad (4)$$

If we assume that $\exp\{(E_m^{endo} - E_m^{exo})/k_B T\} \approx 1$, i.e., $E_m^{endo} \approx E_m^{exo}$, then the ratio of the rate constants under mechanochemical conditions is almost the same as that under conventional conditions. Therefore, no external force along the reaction mode can explain the difference in selectivities between mechanochemical and conventional conditions. The validity of the assumption of $E_m^{endo} \approx E_m^{exo}$ is confirmed later for our target reaction.

Subsequently, we discuss the forces orthogonal to the reaction mode. If the deformation in the direction orthogonal to the reaction mode considerably lowers the reaction barrier, then such a reaction pathway must be mechanochemically favorable. The potential energy E can be expanded around the TS in terms of the reaction coordinate Q_s :

$$E = E_{TS} + \frac{1}{2} \left(\frac{\partial^2 E}{\partial Q_s^2} \right)_{TS} Q_s^2 + \frac{1}{3!} \left(\frac{\partial^3 E}{\partial Q_s^3} \right)_{TS} Q_s^3 + \frac{1}{4!} \left(\frac{\partial^4 E}{\partial Q_s^4} \right)_{TS} Q_s^4 + \dots \quad (5)$$

where E_{TS} is the potential energy at the TS. By the definition, $(\partial^2 E / \partial Q_s^2)_{TS}$ is negative, and $(\partial^4 E / \partial Q_s^4)_{TS}$ is positive. As shown in Figure 2c, the activation energy can be lowered by the deformation when the absolute value of the potential energy curvature $(\partial^2 E / \partial Q_s^2)_{TS}$ becomes smaller. It should be noted that we ignored the change in the higher-order derivatives for simplicity. In this case, the decrease in the activation energy depends on the feasibility of variation in the curvature by deformation in mode α , which can be evaluated by a cubic force constant γ_α

$$\gamma_\alpha = \left[\frac{\partial}{\partial Q_\alpha} \left(\frac{\partial^2 E}{\partial Q_s^2} \right) \right]_{TS} \quad (\alpha = 1, 2, \dots, f_{\text{vib}} - 1) \quad (6)$$

where f_{vib} denotes the vibrational degrees of freedom. Herein, we introduce a cubic effective mode \mathbf{u}_{eff} which is the deformational mode \mathbf{u}_α such that the curvature variation is maximum,

$$\mathbf{u}_{\text{eff}} = \frac{1}{N} \sum_{\alpha=1}^{f_{\text{vib}}-1} \gamma_\alpha \mathbf{u}^\alpha, \quad N = \sqrt{\sum_{\alpha=1}^{f_{\text{vib}}-1} \gamma_\alpha^2} \quad (7)$$

where N denotes a normalization factor, and \mathbf{u}^α is a vibrational vector for mode α . The cubic force constant γ_{eff} for the cubic effective mode \mathbf{u}_{eff} is given by N . γ_{eff} characterizes the maximum curvature variation due to the application of a random force. The difference in γ_{eff} values among the possible reaction pathways should be one of the origins of mechanochemical selectivity.

COMPUTATIONAL METHODS

Employing density functional theory (DFT) calculations, geometry optimizations and vibrational analyses were performed for the reactants, intermediates, TSs, and products in a vacuum and toluene for the two reaction pathways yielding the *endo* and *exo* products. The solvent effect was incorporated using the polarizable continuum model (PCM). Intrinsic reaction coordinate calculations were then carried out to confirm the validity of the obtained TSs. Subsequently, anharmonic vibrational analyses were performed for the TSs to obtain the cubic force constants for the reaction mode and other normal modes. All the DFT calculations were performed at the B3LYP/6-311G(d,p) level of theory using the Gaussian 09, Rev.D.01 program package.¹² Further, as per eq 7, the cubic effective mode \mathbf{u}_{eff} was calculated with its cubic force constant γ_{eff} for each TS to elucidate the changes in the potential energy curve by an external force. Finally, the potential energy surface along the reaction and cubic effective modes was calculated to estimate the activation energies during deformation.

RESULTS AND DISCUSSION

Figure 3 shows the obtained energy diagrams for the two reaction pathways. The activation energy in the *endo*-type path is 0.12 eV lower in a vacuum and 0.13 eV lower in toluene than that for the *exo*-type path. This result is consistent with the experimental results where the *endo* product is preferred even under conventional conditions.⁷

Hereafter, we discuss the mechanochemical effect on activation energies in a vacuum. First, we investigated the impact of an external force along the reaction mode, with respect to stereoselectivity. As previously mentioned, if we assume that $\exp\{(E_m^{endo} - E_m^{exo})/k_B T\} \approx 1$, then the stereoselectivities should be approximately the same between mechanochemical and conventional conditions. This assumption needs to be validated. The magnitude of the applied external force is assumed to be the same for each pathway. We then calculated $\exp\{(E_m^{endo} - E_m^{exo})/k_B T\}$ and found that the

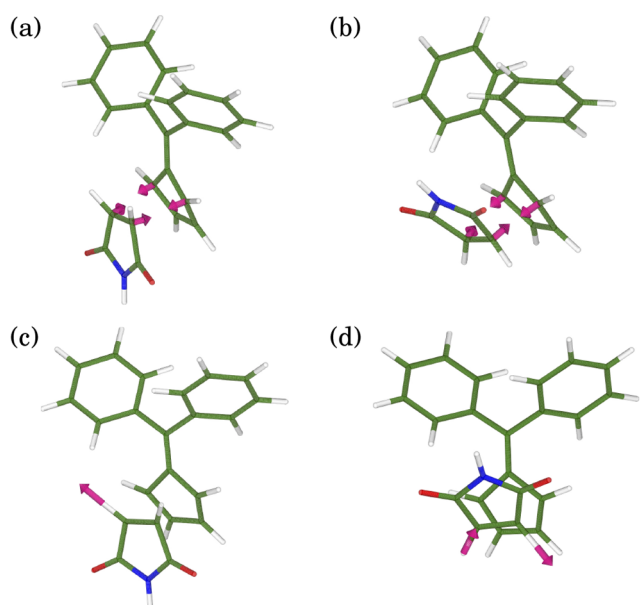


Figure 4. Vibrational vectors for the (a) *endo*-type and (b) *exo*-type reaction modes as well as the (c) *endo*-type and (d) *exo*-type cubic effective modes.

value is approximately 1.0 within the actual range of the force, which corresponds to a force of subnano Newtons. Thus, for the present Diels–Alder reaction, any external force along the reaction mode does not significantly contribute to mechanochemical stereoselectivity. Details are described in the [Supporting Information](#).

Further, we examined the effect of an external force in the direction orthogonal to the reaction mode. At the obtained TSs for the two pathways, we calculated the cubic force constants for the reaction mode and other normal modes and then obtained the effective cubic force constants. As a result, we determined that γ_{eff} in the *endo* case (1.25×10^{-2} Hartree·amu $^{-3/2}$ ·Bohr $^{-3}$) is greater than that in the *exo* case (1.04×10^{-2} Hartree·amu $^{-3/2}$ ·Bohr $^{-3}$). This implied that the curvature at the TS in the *endo* case is varied more by external force than that in the *exo* case. In general, a cubic force constant can be rewritten as the sum of its primary term and its mixing term based on the third-order perturbation theory. The primary term depends only on the total electron density in the ground state. In contrast, the mixing term depends on the excited states as well as the ground state, in which their energy gaps are denominators. In the *endo* path, the rings of the reactants overlap largely. This increases the orbital interaction and thus widens the energy gap between occupied and unoccupied

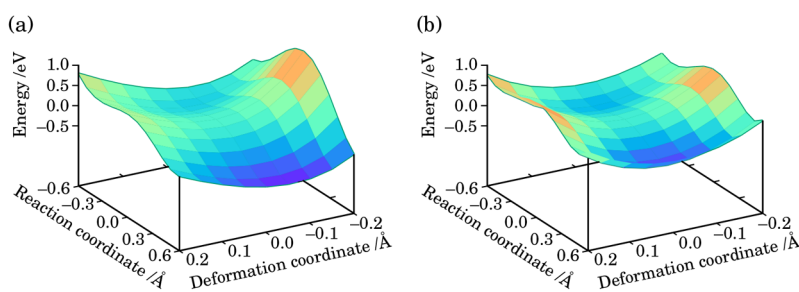


Figure 5. Potential energy surfaces along the reaction and cubic effective modes in the (a) *endo*-type and (b) *exo*-type pathways.

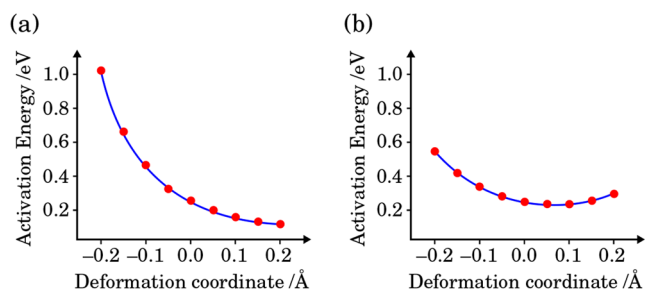


Figure 6. Activation energies when deformed along the cubic effective modes in the (a) *endo*-type and (b) *exo*-type pathways.

molecular orbitals, stabilizing the transition state. Due to such a wide gap between ground and excited states, the mixing term is minor in the *endo* case. This is one of the plausible reasons the effective cubic force constants and cubic effective modes differ between *endo* and *exo*.

[Figure 4](#) shows the obtained reaction modes and cubic effective modes. For reaction modes, the diene site of diphenylfulvene and dienophilic site of maleimide approach each other. In contrast, unexpectedly, the cubic effective modes consist of a few C–H stretching modes of maleimide in both the pathways. One plausible reason for this is that the C–H stretching modes assist in the conversion of $sp^2 \rightarrow sp^3$ in carbons around the reactive regions. If these modes are partially excited during mechanical grinding, then the curvatures change considerably.

To determine how easily an external force changes curvature, potential energy surfaces along the reaction and cubic effective modes were calculated, as shown in [Figure 5](#). When the molecular structure is deformed along the cubic effective mode, the curvature in the *endo*-type pathway changes more extensively than that in the *exo*-type pathway. This implies that the activation energy is also more variable in the *endo* case, owing to the difference in the γ_{eff} values between the two pathways.

Finally, we estimated the activation energies for each values of the deformational coordinates based on the obtained potential energy surfaces, as shown in [Figure 6](#). In the *endo*-type pathway, the reaction barrier is significantly decreased by deformation. In contrast, in the *exo*-type pathway, the reaction barrier did not change as significantly. This result clearly explains the experimentally observed stereoselectivity; under mechanochemical conditions, the yield of the *endo* product is higher than that of the *exo* product.⁷

■ CONCLUSION

We theoretically elucidated how a mechanical action changes the reaction barriers and thereby influences stereoselectivity in the Diels–Alder reaction of diphenylfulvene and maleimide. Particularly in the endotype reaction pathway, it was found that the potential energy curvature at the transition state is easily altered by external forces, resulting in a reduction of the reaction barrier. Such a mechanochemically favorable pathway can be predicted from the cubic force constants for the reaction mode and the other modes orthogonal to the reaction mode.

■ ACKNOWLEDGMENTS

We used the supercomputer of ACCMS, Kyoto University; the SuperComputer System, Institute for Chemical Research, Kyoto University; the supercomputer system at the information initiative center, Hokkaido University, Sapporo, Japan. This work was supported by JSPS Summer Program; Special

Project by Institute for Molecular Science (IMS program 22-IMS-C065).

■ REFERENCES

- (1) Wang, G.-W. Mechanochemical organic synthesis. *Chem. Soc. Rev.* **2013**, *42*, 7668–7700.
- (2) Beyer, M. K.; Clausen-Schaumann, H. Mechanochemistry: The mechanical activation of covalent bonds. *Chem. Rev.* **2005**, *105*, 2921–2948.
- (3) Potisek, S. L.; Davis, D. A.; Sottos, N. R.; White, S. R.; Moore, J. S. Mechanophore-linked addition polymers. *J. Am. Chem. Soc.* **2007**, *129*, 13808–13809.
- (4) Baron, M. Towards a greener pharmacy by more eco design. *Waste Biomass Valorization* **2012**, *3*, 395–407.
- (5) Wang, G.-W.; Komatsu, K.; Murata, Y.; Shiro, M. Synthesis and X-ray structure of dumb-bell-shaped C₁₂₀. *Nature* **1997**, *387*, 583–586.
- (6) Hickenboth, C. R.; Moore, J. S.; White, S. R.; Sottos, N. R.; Baudry, J.; Wilson, S. R. Biasing reaction pathways with mechanical force. *Nature* **2007**, *446*, 423–427.
- (7) Gonnet, L.; Chamayou, A.; André-Barrès, C.; Micheau, J.-C.; Guidetti, B.; Sato, T.; Baron, M.; Baltas, M.; Calvet, R. Elucidation of the Diels–Alder Reaction Kinetics between Diphenylfulvene and Maleimide by Mechanochemistry and in Solution. *ACS Sustain. Chem. Eng.* **2021**, *9*, 4453–4462.
- (8) Hernández, J. G.; Bolm, C. Altering product selectivity by mechanochemistry. *J. Org. Chem.* **2017**, *82*, 4007–4019.
- (9) Luty, T.; Ordon, P.; Eckhardt, C. J. A model for mechanochemical transformations: Applications to molecular hardness, instabilities, and shock initiation of reaction. *J. Chem. Phys.* **2002**, *117*, 1775–1785.
- (10) Ribas-Arino, J.; Shiga, M.; Marx, D. Understanding covalent mechanochemistry. *Angew. Chem., Int. Ed.* **2009**, *48*, 4190–4193.
- (11) Haruta, N.; de Oliveira, P. F. M.; Sato, T.; Tanaka, K.; Baron, M. Force-induced dissolution of imaginary mode in mechanochemical reaction: Dibenzophenazine synthesis. *J. Phys. Chem. C* **2019**, *123*, 21581–21587.
- (12) Frisch, M. J.; Trucks, G. W.; Schlegel, H. B.; Scuseria, G. E.; Robb, M. A.; Cheeseman, J. R.; Scalmani, G.; Barone, V.; Mennucci, B.; Petersson, G. A. et al. *Gaussian 09 Revision D.01.*; Gaussian Inc.: Wallingford, CT, 2009.